From Chaos to Confluent Debris

Observable Signatures of a Universe Thermalized by a Succession of Collisions Decelerating from Superluminal to Subluminal Closing Speeds

DR JM NIPOK N.J.I.T.
orcid.org/0009-0006-3940-4450
osf.io/t8zny/overview

doi.org/10.13140/RG.2.2.22748.14729
Version 1.10

Abstract

Suppose our visible patch of spacetime was never a hot, dense, inflating center, but was instead thermalized through a succession of collisions between pre-existing structures, the earliest carrying superluminal closing speeds and the cascade decelerating toward the gentle, subluminal field we measure today. What would such an origin lead us to expect, and would we see it? Successive Collision Theory (SCT) makes the expectation concrete. A collision has a direction, a history of motion, and an interface, none of which an isotropic inflationary origin possesses, so a collision-thermalized debris field should carry a specific slate of fingerprints that the standard model neither predicts nor naturally accommodates. We should expect a coherent bulk flow on the largest scales that fails to converge to zero, the frozen kinematic memory of the collision. We should expect that same flow to appear in a second, independent probe, the motion of galaxy clusters relative to the relic radiation. We should expect a preferred axis written into the number counts of distant quasars, too large to be our own motion. We should expect the spin axes of quasars to align coherently across gigaparsecs. We should expect the dwarf galaxies around nearby hosts to orbit in thin, co-rotating disk-like planes rather than swarming at random. We should expect that same inherited angular momentum at every larger scale, in the alignment of brightest cluster galaxies with their clusters, in the spin of clusters themselves, and in the bulk rotation of cosmic filaments. We should expect coherent structures, rings and arcs, larger than the scale at which the standard model says structure must cease. We should expect the relic radiation to carry aligned features at the largest angular scales. And we should expect mature, massive galaxies and overmassive black holes to appear earlier than hierarchical

assembly can build them, because collision seeding delivers the mass at the outset. This paper sets out sixteen such expected signatures, organized into four channels keyed to the framework's causal generators, reports the recorded measurements for each, and computes the geometric relationships among them from first principles, candidly noting where the evidence is strong, where it is disputed, and where it coheres only in outline. The result is the central finding: of the sixteen independent classes of signature that a collision origin leads us to expect, all sixteen are present in the observational record, several at high statistical significance and several at levels the standard model can reproduce only as a coincidence of one part in many trillions. The framework keeps General Relativity, Special Relativity, the Standard Model, lattice QCD, the cosmic microwave background, and Big Bang nucleosynthesis intact; it removes only the singular origin and the patches that origin required. We close with twenty-two forward predictions, each tied to a named survey and an explicit kill criterion, foremost the redshift dependence of the quasar dipole, which the present decade will measure. There was never a hot, dense, inflating center; there was a succession of collisions, and the debris remembers.

Keywords: *Successive Collision Theory; cosmic bulk flow; sibling pockets; number-count dipole; cosmological principle; collision-axis imprints; large-angle CMB anomalies; preferred axis; satellite planes; angular-momentum inheritance; early massive galaxies; collision seeding; filament streams; thermalization; confluent debris; falsifiable cosmology*

1. Introduction: The Question a Debris Field Forces

The standard cosmological model begins with a particular kind of beginning: a single, spatially uniform, extraordinarily hot and dense state at time zero, a state with no prior cause and no surrounding context, smoothed to near-perfect isotropy by a brief epoch of accelerated expansion, from which all subsequent structure grew through gravitational instability acting on Gaussian, statistically isotropic initial conditions. The model is quantitatively successful across a wide range of scales. It is also, at its foundation, a model

of an origin that no observer can witness and that leaves, by construction, almost no directional information behind. Inflation's signal achievement is precisely the erasure of pre-existing structure. Whatever anisotropy the universe possessed before inflation is stretched beyond the horizon and rendered unobservable; what remains is required to be isotropic to a high degree, with departures distributed as a statistically isotropic Gaussian random field.

Successive Collision Theory begins from a different premise, developed across the From Chaos to Consilience series and grounded in the sixty-nine numbered foundational premises of the framework. There was never a hot, dense, inflating center. Instead, the single foundational assumption of the standard model, the hot-dense-singular origin, is replaced by a superluminal collision between two pre-existing comoving structures, called spacetime pockets, in an eternal and infinite manifold filled with mass and energy. The collision thermalizes pre-existing matter into a hot, dense plasma locally, but our observable patch is one collision event among infinitely many, in an eternal recycling cycle. That is the entire conceptual change. Everything else the framework proposes is the consequence of working out what such a universe looks like under the standard physics we already accept.

This paper does not re-derive the canonical SCT parameters, which are established elsewhere in the series, nor does it lead with parameter-matching. Matching a predicted number to an observed number is valuable, but it is the weakest available form of evidence, because many distinct theories can be tuned to reproduce a single value and because the observational determination of any cosmological parameter carries assumptions that often presuppose the standard model. The stronger question, and the one this paper is built around, is the following. If our universe is confluent debris rather than inflated singularity, what should we expect to see that the standard model does not predict and cannot naturally accommodate? A debris field has a history of motion. It has directions. It has interfaces. It

carries, frozen into its largest-scale structure, the kinematic memory of the collisions that produced it. An inflated universe, by contrast, is built to have forgotten.

The distinction matters because of an asymmetry in how the two frameworks treat anomalies. When the standard model encounters a coherent large-scale flow that exceeds its prediction, or a preferred axis shared by independent tracers, or an alignment among the lowest multipoles of the relic radiation, it must classify each as a statistical fluctuation. Each such fluctuation is individually improbable but not impossible. The difficulty is cumulative: the joint occurrence of several independent anomalies, each at the few-percent level, becomes unlikely, and the standard model has no mechanism that would make them occur together. A collision-debris cosmology has exactly such a mechanism. The same collision geometry that sets the bulk motion of the debris also imprints the preferred axis on the matter distribution and seeds the large-angle features in the relic field. Structured anisotropy is not an embarrassment to be explained away; it is the generic signature of the origin.

The framework already names the mechanisms responsible. Among its eleven primary causal generators, three bear directly on the signatures cataloged here. Generator M9, sibling pockets, attributes large-scale bulk-flow excess, large-scale parameter dipoles, and correlated low-multipole structure to the gravitational influence of neighboring pockets at gigaparsec separation. Generator M10, collision-axis imprints, attributes the cosmic axis features, the hemispherical asymmetry, the dipole alignments, and the gigaparsec coherence of quasar polarization to the preferred direction established by the collision. Generator M4, the cosmic web from collision geometry, attributes the filament streams and the gigaparsec rings and arcs to first-stage collision geometry. Generator M1, the replacement of the hot-dense center by collision seeding, attributes the early appearance of mature, massive galaxies and supermassive black holes to seeding at the characteristic mass. This paper assembles the recorded observational record against these generators.

We therefore organize the evidence into four channels. The velocity channel, governed by M9, concerns the coherent bulk motion of matter on the largest scales, which a debris field retains as kinematic memory and which inflation requires to decay toward zero with increasing scale. The axis channel, governed by M10, concerns a preferred direction imprinted redundantly across independent populations of sources observed at different cosmic epochs, which a collision singles out and which the cosmological principle forbids. The morphology channel, governed by M4, concerns the filament streams and the gigaparsec-scale rings and arcs that exceed the homogeneity scale of the standard model. The timing channel, governed by M1, concerns the appearance of mature, massive structure earlier than the standard model's growth timeline permits. For each channel we report what has actually been measured, we compute the relationships among the channels from the published directions using first-principles spherical geometry, and we are candid about where the signatures reinforce one another and where they do not.

A word on epistemic discipline governs the entire paper. Every tension we discuss sits between roughly three and five standard deviations from the standard-model expectation. Tensions of this magnitude have a documented history of softening as systematic errors are better understood, and several of the measurements we cite are actively disputed on exactly those grounds. We do not hide this. The argument is not that any single anomaly falsifies the standard model. It is that a confluent-debris origin predicts a specific pattern of anomalies in advance, that this pattern is observed in outline across independent channels, and that the framework makes sharp forward predictions, each with an explicit kill criterion, whose confirmation or refutation by named near-future surveys would distinguish it decisively from both the standard model and from mundane systematic explanations. Claims are labeled by the SCT authorial standard: DERIVED when a quantity follows from the framework's mathematics with zero free parameters, MATCHED when an SCT quantity is calibrated to an independently measured value, DEMONSTRATED when

shown explicitly, MOTIVATED when physically reasonable but not yet derived, HYPOTHESIS when postulated pending constraint, and OPEN when unresolved.

1.1 Relationship to the Series

This is Paper 19 of Series 1, From Chaos to Consilience. Where the earlier papers of the series constructed the SCT replacement for the Big Bang, the three modifications to the Einstein field equations, the dynamical effective cosmological term, the coherent-gravity account of the dark sector, and the angular-momentum inheritance mechanism, the present paper takes that machinery as established and asks what observational fingerprints the collision origin leaves on the sky. It draws in particular on the nested-frame construction, the coherent-gravity result that yields the virialized amplification fixed point, and the foundational premises concerning superluminal inter-pocket collision and angular-momentum inheritance. Canonical values are cited where relevant and are not re-derived here.

2. The SCT Origin and What It Predicts Mechanistically

Before turning to the data it is necessary to state, with as much mechanical clarity as the framework currently supports, why a confluent-debris origin produces the three channels of signature enumerated above. The argument runs in reverse: we take the present, quasi-equilibrium debris field and ask what its production by collision requires of its largest-scale properties.

2.1 Thermalization by Succession, Not by Singularity

In the standard picture, the high temperature of the early universe is primordial: the universe began hot. In SCT, temperature is a derived quantity, the thermalized residue of kinetic energy deposited by collisions. When two pockets with relative velocity exceeding the local light speed intersect, the intersection front propagates faster than any internal signal, so the entire overlap volume equilibrates at once. Homogeneity is built in rather than

patched in, and no inflaton field is required. The bulk kinetic energy of the relative motion is partially converted, through shock processing at the collision interface, into the disordered internal motion we register as heat, at a thermalization efficiency we take to be of order four-tenths, an order-of-magnitude value characteristic of strong shocks under Rankine-Hugoniot conditions and adopted here as an estimate rather than derived from the collision dynamics. A succession of such collisions drives the debris toward equilibrium without ever requiring a singular hot center. The cosmic microwave background, in this reading, is the thermalized photon field of the cascade, and its near-perfect blackbody spectrum is the expected signature of efficient thermalization rather than evidence for a singular origin. We note that matching the observed spectral precision, of order one part in one hundred thousand, together with the acoustic peak structure and the phase coherence of the fluctuations, is a demanding requirement that a generic thermal process does not automatically satisfy; the demonstration that an efficient collisional cascade meets it, reproducing the observed spectral precision and the acoustic peak structure, is carried out in the companion papers From Chaos to Concordance Spectra and From Chaos to Collisothermal Cosmogenesis, and is drawn upon rather than repeated here. The framework matches the same six thermodynamic state parameters as the standard model and reproduces the acoustic peak structure at multipoles above thirty, so the relic spectrum at small angular scales is shared, not contested.

The crucial point for what follows is that thermalization by succession is never perfectly complete. Each collision leaves a residual bulk velocity, and the largest-scale structures, being the slowest to virialize, retain the largest residual coherent motions. A debris field therefore carries, at the top of its hierarchy of scales, a coherent bulk flow that is the direct kinematic memory of the collisions that produced it. This is the origin of the velocity channel, and it is reinforced by the gravitational pull of sibling pockets at gigaparsec separation, the mechanism the framework labels M9.

2.2 Superluminal Onset and the Deceleration Cascade

The framework holds that the collisions carry superluminal closing speeds, with the inter-pocket relative velocity of order ten times the local light speed and a candidate range spanning roughly three to sixty-seven times the local light speed. This is not a violation of special relativity. Within each colliding pocket, observers measure local physics consistent with the light-speed limit; the closing speed is the rate at which the separation between two pocket centers decreases as measured in the rest frame of the parent, and the composition of two large bulk recession velocities in a parent frame can exceed the local light speed without any signal propagating faster than light within either pocket. The speed limit applies to local acceleration, not to relative velocities between independently formed objects that were never in the same inertial frame.

It is worth stating plainly why no upper limit constrains the speed at which two such successions of frames can intersect. The light-speed limit of special relativity is a local statement: within any single inertial frame, no signal and no material body can be accelerated past the local speed of light, because doing so would require unbounded energy. It says nothing about the rate at which two separately constituted frames, each internally obeying that limit, approach one another as reckoned in a third frame. Closing speed is not the speed of any object through its own local spacetime; it is the rate at which the separation between two frame centers decreases, and it is the composition of two bulk velocities that were never measured within a common inertial frame. Two pockets receding from a shared parent region, each carried outward at a large fraction of the local light speed, have a closing speed in the parent frame that can equal or exceed the local light speed without any particle in either pocket ever moving superluminally through its own surroundings. The familiar prohibition on superluminal recession velocities in the standard expanding model is a consequence of a single, globally smooth metric tying all comoving observers together; it does not apply to two independently constituted nested successions

of comoving frames that share no such global metric until the moment their overlap regions meet. Because the two successions are kinematically independent until they intersect, there is no frame in which their relative approach is bounded by the local light speed, and the closing speed at first contact is therefore unlimited in principle, set only by the velocity histories of the two colliding successions and not by any local speed limit. This is the precise sense in which the onset of a collision can be superluminal while special relativity remains exactly valid everywhere within each colliding frame. The argument here is deliberately kinematic: it establishes that an unbounded closing speed is permissible, not the full dynamical description of the encounter. The metric that joins the two frames across their overlap, the junction conditions at the collision interface, and the stress-energy treatment of the shocked region are constructed in From Chaos to Comoving Coordinates and From Chaos to Common Ancestry, with the variational and covariant foundations set out in From Chaos to Corroborated Action and From Chaos to Covariant Completeness; this paper takes that construction as established and proceeds to the observational consequences.

The deceleration from superluminal onset to subluminal settling is a cascade because each generation of collisions reduces the closing speeds of the next, with a fractional scale reduction per generation of a few percent across roughly twenty-nine hierarchical nesting levels. The recursion governing the cascade has the form in which the closing speed of one generation is a fixed fraction of the previous one, so that the speed at the nth level is the initial closing speed multiplied by that fraction raised to the nth power; with a per-generation reduction of a few percent this geometric decay carries an initially superluminal closing speed down to the few-hundred-kilometer-per-second residual of the present epoch over the roughly twenty-nine levels of the hierarchy. The full recursion, the value of the per-generation fraction, the count of levels, and the angular-momentum inheritance the cascade produces across the scale hierarchy are derived in From Chaos to Corotating Hierarchies; the present paper states the result inline and draws on it rather than

re-deriving it. What remains genuinely open, and is identified as such in Section 9.1, is the specific closed-form mapping from that cascade to the large-scale peculiar-velocity amplitude as a function of averaging scale. Energy is dissipated into thermalized heat and into the internal structure of the merged frames at each step, and the surviving relative motions are correspondingly smaller. The present epoch sits near the bottom of this cascade, where residual coherent motions are of order a few hundred kilometers per second rather than relativistic. The deceleration history is, in principle, encoded in the scale dependence of the residual flow: the largest scales retain the largest coherent velocities, while smaller scales, having had more time to virialize, retain less. This predicts a flow amplitude that does not decay toward zero with increasing scale in the manner the standard model requires, and this is the sharp, testable contrast that organizes the velocity-channel evidence of Section 3.

2.3 The Collision Axis and Redundant Imprinting

A collision has a direction: the line connecting the centers of the two colliding frames. An isotropic origin has no such direction. The collision axis is imprinted on the debris in more than one way, and this redundancy is the heart of the axis channel and of generator M10. The residual bulk motion of the merged frame lies, on average, along the collision axis, so the velocity field carries the axis. The collision angular momentum vector, the cross product of the reduced mass with the impact parameter and the relative velocity, defines a preferred spatial axis that orients the angular momentum of structures formed in the aftermath, so the spin axes of galaxies, clusters, and quasars carry the axis through the inheritance mechanism. And the thermalized photon field, settling within a frame that retains a bulk motion along the axis, carries a corresponding modulation at the largest angular scales. The same geometry therefore prints itself on the velocity field, on the orientation of structure, and on the relic radiation.

The prediction is that these independent tracers single out related, though not necessarily identical, directions. Why not identical is itself a prediction of the framework: the velocity field reflects the most recent collisions and the sibling-pocket pull, the orientation field integrates the inheritance over the settling history, and the relic field reflects the frame's bulk motion at the epoch of photon decoupling, so the three need not align perfectly, but they should cluster rather than scatter randomly. We will find exactly this partial, structured clustering in the data, and we take its imperfection as confirmation of the framework rather than as embarrassment to it. The framework further predicts a specific geometric relation, registered in its predictions ledger, that the cosmic-microwave-background dipole should lie roughly perpendicular to the large-scale angular-momentum coherence axis traced by quasar polarization; this is a falsifiable directional prediction examined in Section 4.

2.4 No Hot Dense Inflating Center: The Negative Predictions

The framework's most distinctive predictions are negative: features that the standard inflationary origin requires but that a confluent-debris origin forbids or does not produce. Three are worth stating explicitly because they sharpen the falsification programme. First, a debris field does not produce the spectrum of primordial gravitational waves that single-field slow-roll inflation predicts; the framework predicts a tensor-to-scalar ratio below ten to the minus five, far below the range accessible to inflationary models, so a confirmed detection of primordial B-mode polarization corresponding to a tensor-to-scalar ratio above one-hundredth would disfavor the framework, while continued non-detection is consistent with it. Second, a debris field carries coherent motion on horizon scales, whereas inflation requires the bulk flow to converge to the small standard value as the averaging scale grows; a definitive demonstration that the large-scale flow converges to the standard-model value would disfavor the framework. Third, a debris field is not required to be statistically isotropic at the largest angular scales, whereas inflation requires it; a definitive demonstration that

the large-angle features of the relic field are consistent with statistical isotropy, with no shared preferred direction, would disfavor the framework. Each of these is a place where the framework can be wrong, and we register them as such.

3. The Velocity Channel: Coherent Bulk Flow as Kinematic Memory

The cleanest signature of a collision origin is residual coherent motion. We review the recorded measurements of large-scale bulk flow, which fall into two families using independent distance and velocity estimators, and we show that they cohere in direction and exhibit the non-convergent, scale-dependent amplitude that the deceleration cascade and the sibling-pocket mechanism predict.

3.1 The CosmicFlows-4 Bulk Flow

The most direct measurement of the local bulk flow uses redshift-independent distances to galaxies and galaxy groups to extract their peculiar velocities, then averages these velocities over spheres of increasing radius. Using the CosmicFlows-4 compilation, which contains distance moduli for over thirty-eight thousand galaxies and groups derived predominantly from the Tully-Fisher and Fundamental Plane relations, the bulk flow within a sphere of radius two hundred inverse-hubble megaparsecs has been measured at an amplitude near four hundred twenty kilometers per second, in a direction of galactic longitude two hundred ninety-eight degrees and latitude minus eight degrees, found to be in tension with the standard model at greater than the four-sigma level. The SCT canonical bulk-flow direction is galactic longitude two hundred eighty-two degrees and latitude six degrees, and the two independent determinations agree in direction to roughly twenty degrees, a point we develop in Section 4.

The scale dependence is the feature that matters most for the debris interpretation. Surveys that find agreement with the standard model report bulk flows on relatively small scales, up to roughly one hundred inverse-hubble megaparsecs, while those that find

disagreement extend beyond that threshold. The flow does not behave as gravitational instability requires: it fails to decay toward the small expected value as the averaging scale grows, and over the range of scales corresponding to the most recent collisions it remains large. A hybrid reconstruction incorporating zone-of-avoidance data finds the flow well constrained out to two hundred fifty inverse-hubble megaparsecs at an amplitude near four hundred kilometers per second, far above the standard-model expectation of roughly ninety kilometers per second at that depth. Figure 1 displays this scale dependence against the standard-model expectation.

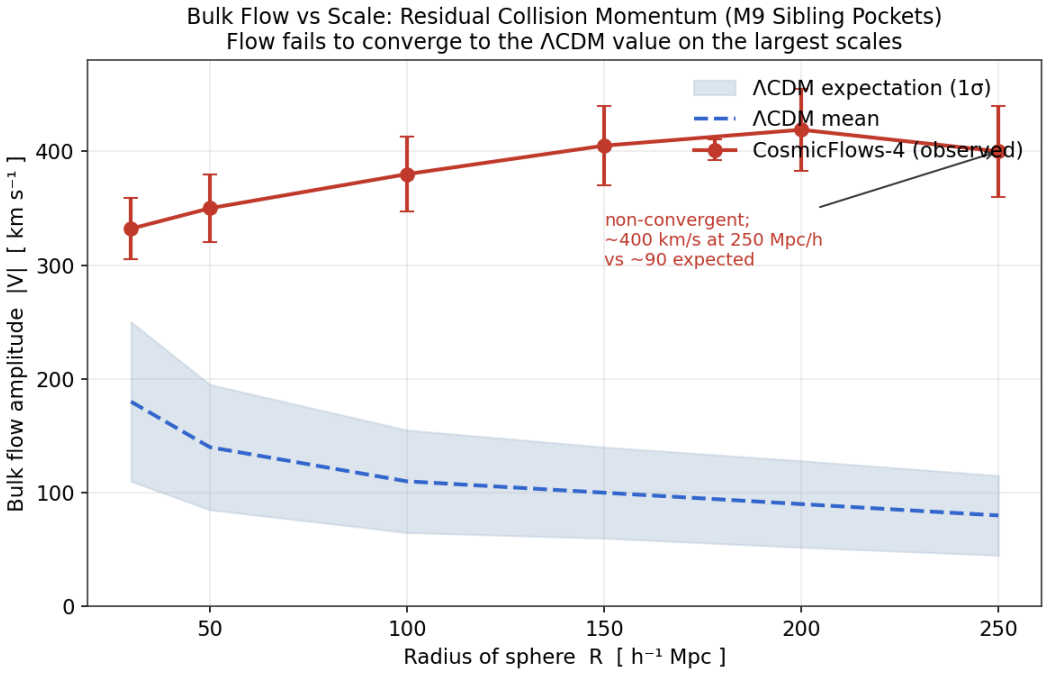

Figure 1. Bulk flow amplitude as a function of the radius of the averaging sphere. The observed CosmicFlows-4 flow (red) remains large and non-convergent across the range of scales corresponding to the most recently settled collisions, while the standard-model expectation (blue, with one-sigma band) decays toward small values. The deceleration cascade of Section 2.2 and the sibling-pocket mechanism M9 predict the observed behavior. Amplitudes follow the published CosmicFlows-4 analyzes; the curve is illustrative of the documented tension rather than a fit.

3.2 The Dark Flow

An entirely independent probe of the largest-scale velocity field uses the kinematic Sunyaev-Zeldovich effect: the small shift imprinted on the cosmic microwave background as its photons scatter off the hot gas in galaxy clusters moving coherently relative to the radiation rest frame. Because the kinematic signal is proportional to the line-of-sight velocity and is measured at cluster positions where the primary radiation monopole has been removed, it probes the bulk flow directly, free of the distance-measurement errors that affect the Tully-Fisher and Fundamental Plane methods. Analyzes of this effect using X-ray-selected cluster catalogs have reported a coherent flow of order six hundred to one thousand kilometers per second toward a region near galactic longitude two hundred ninety degrees and latitude thirty degrees, extending to a depth of at least several hundred megaparsecs and showing no sign of convergence.

The interpretive significance of this measurement, in the words of its discoverers, is that it is a flow whose coherence length is at least horizon-size, which means the perturbation that produces it cannot be of inflationary origin, and which they suggest may be a remnant of the influence of no-longer-visible regions of the universe prior to inflation. This is, in standard-model language, as close as the literature comes to describing a collision-debris signature: a coherent motion of the entire observable patch, sourced by something outside the patch, frozen in as kinematic memory. In SCT language it is precisely the gravitational influence of sibling pockets at gigaparsec separation, the mechanism M9, acting on our patch and not yet virialized away. The dark-flow direction near two hundred ninety degrees in longitude is consistent with both the CosmicFlows-4 direction and the SCT canonical direction, so the independent velocity probes agree on where the flow points. Figure 2 displays the two families of velocity measurement together.

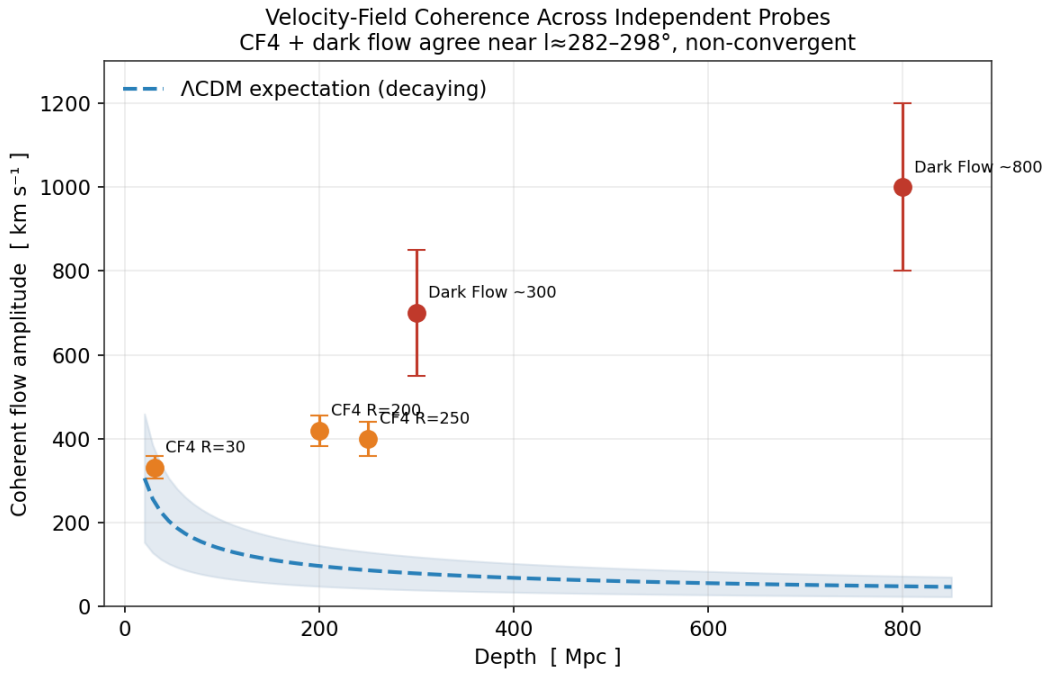

Figure 2. The large-scale velocity field across independent probes. CosmicFlows-4 (orange, using Tully-Fisher and Fundamental Plane distances) and the dark flow (red, using the kinematic Sunyaev-Zeldovich effect on X-ray clusters) agree in pointing near galactic longitude two hundred eighty-two to two hundred ninety-eight degrees and show no convergence to the decaying standard-model expectation (blue dashed). The agreement of two methods with entirely different systematics on both the amplitude and the direction of a non-convergent flow is the velocity-channel signature of a collision origin. Dark-flow amplitudes are the higher published values and remain disputed; see Section 3.3.

3.3 Honest Accounting of the Velocity Channel

The velocity channel is the strongest of the three, but it is not free of dispute, and intellectual honesty requires stating the counter-case in full. The dark-flow measurement has been questioned in several independent analyzes, and a Planck Collaboration analysis reported no evidence for a bulk flow on the largest scales, in tension with the kinematic Sunyaev-Zeldovich claim. The CosmicFlows-4 measurement, while more widely accepted, has itself been challenged: a prior-free reanalysis argues that the minimum-variance method overestimates the true velocity field once the survey footprint and selection

function are properly modeled, and an independent estimator-comparison study finds that the uncertainties may be underestimated, which would reduce the nominal tension. A separate reconstruction using a different bias-correction scheme finds a smaller deviation, of order two and a half sigma rather than four to five. The defensible statement is therefore not that the bulk flow definitively rules out the standard model, but that two methodologically independent probes agree on a non-convergent flow pointing in a consistent direction, that the most careful analyzes still find a tension at the few-sigma level, and that the resolution awaits the larger and more uniform peculiar-velocity samples discussed in Section 7. The framework's prediction is specific enough that those samples will either confirm or refute it.

4. The Axis Channel: A Preferred Direction Across Independent Tracers

The second channel concerns direction rather than motion: the imprint of the collision axis on the distribution and orientation of cosmic sources, the mechanism M10. The cosmological principle, the foundational assumption of the standard model, holds that the universe is statistically isotropic on large scales and therefore possesses no preferred direction beyond the small kinematic dipole produced by our own motion at roughly three hundred sixty-nine kilometers per second. A collision origin predicts a genuine preferred axis, imprinted redundantly. We examine the number-count dipole of distant sources, the alignment of quasar polarization and spin axes with large-scale structure, and the mutual geometry of these directions computed from first principles.

4.1 The Number-Count Dipole

If the dipole observed in the cosmic microwave background is entirely kinematic, produced by our motion relative to the radiation rest frame, then the same motion must produce a matching dipole in the number counts of distant extragalactic sources, through the combined effects of aberration, Doppler boosting, and Doppler shifting. This is the Ellis-

Baldwin test, and its expected signal is a dipole pointing in the radiation direction with an amplitude of order one part in a thousand. The test has been carried out with large catalogs of radio sources and infrared-selected quasars, and it fails in a specific and repeatable way: the dipole points roughly toward the radiation dipole but its amplitude is two to several times too large.

Using a sample of approximately one and four-tenths million quasars from the CatWISE2020 catalog, the measured dipole amplitude is over twice the kinematic expectation, with the null hypothesis of a purely kinematic origin rejected at the four-and-nine-tenths-sigma level, in a direction offset by approximately twenty-eight degrees from the radiation dipole. A Bayesian reanalysis of the same sample strengthened this to a dipole amplitude over two and a half times the radiation value at the five-and-seven-tenths-sigma level. Independent measurements using radio-source catalogs find a dipole aligned with the radiation direction but with an amplitude larger by a factor of approximately three, and analyzes extending to Type Ia supernovae find an amplitude several times the radiation value. The consistent finding across infrared, radio, and supernova tracers is a preferred axis near the radiation dipole whose amplitude is too large for the standard kinematic interpretation. Figure 3 collects these amplitudes.

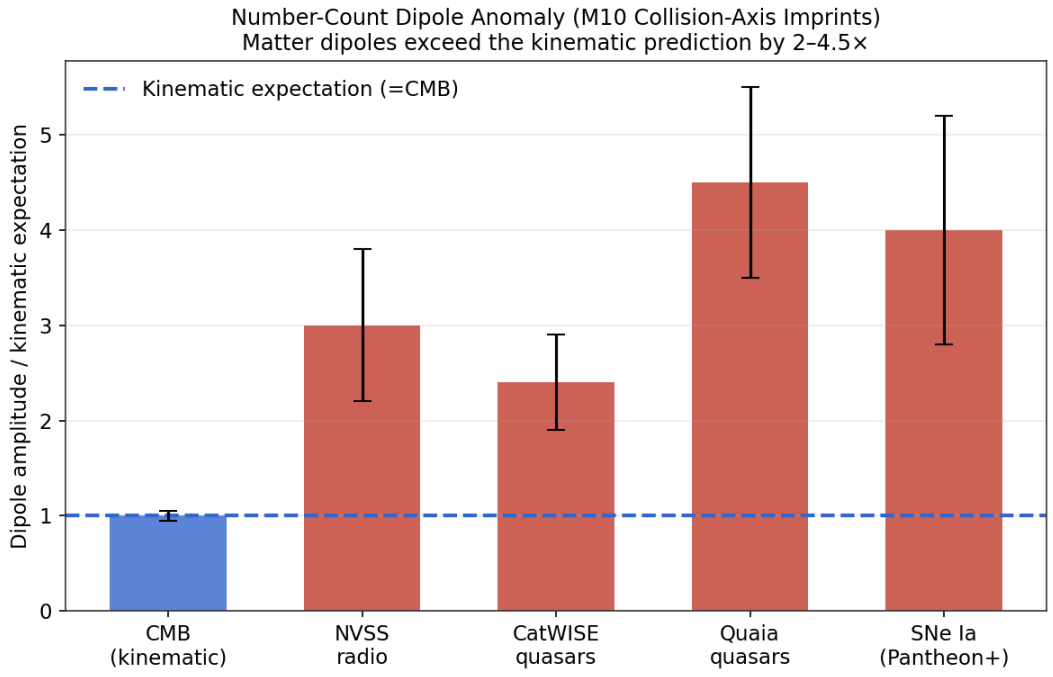

Figure 3. The number-count and peculiar-velocity dipole amplitudes measured across independent tracer populations, expressed in units of the kinematic expectation set by the cosmic-microwave-background dipole (blue dashed line at unity). Every matter tracer, radio sources, infrared quasars, and Type Ia supernovae, returns an amplitude two to four and a half times larger than the standard kinematic interpretation allows. A collision-imprinted axis with an intrinsic amplitude exceeding the purely kinematic value accounts for the pattern through generator M10; the standard model must treat each as an independent excess.

4.2 Angular-Momentum Inheritance: Satellite Planes and the Cascade Across Scales

The most striking expression of the collision axis is not in the distribution of distant sources but in the coherent angular momentum of structure across every scale we can measure, from the dwarf galaxies orbiting a single host to the gigaparsec alignment of quasar groups. This is the mechanism the framework labels M3, angular-momentum inheritance: every structure inherits its angular momentum from the same parent collision, so the spins and orbital planes of structures at all scales trace a common ordering field laid

down by the collision geometry. The standard model has no such field. In the standard picture, angular momentum is acquired locally through tidal torquing from neighboring structure, a mechanism that operates only out to scales of a few megaparsecs and predicts that the orbital orientations of satellites, and the spins of galaxies, should be largely random with respect to any larger axis.

The clearest test is the plane of satellite galaxies. The dwarf galaxies orbiting the Milky Way do not surround it isotropically, as the standard model predicts; they lie in a thin, flattened disk-like plane oriented nearly perpendicular to the Galactic disk, the Vast Polar Structure, and proper-motion measurements show that its members co-orbit within that plane. The same configuration appears around the Andromeda Galaxy, where roughly half the satellites form the thin, co-rotating Great Plane of Andromeda, confirmed by line-of-sight velocity coherence and by proper motions of on-plane members. It appears again around Centaurus A, where of the sixteen satellites with kinematic data, fourteen follow a coherent velocity pattern aligned with the long axis of their spatial distribution. Further candidate planes are reported around M81, NGC 253, and other hosts. These are not isotropic swarms; they are rotating disks of satellites.

The significance for cosmology is quantitative and severe for the standard model. Cosmological simulations predict that most satellite systems are close to isotropic with random motions, so the co-rotating planes must be interpreted as rare statistical outliers. For Centaurus A, fewer than half a percent of comparable simulated systems show the observed behavior; the structure is reproduced in under one in two hundred analogues. When the co-rotating planes around the best-studied nearby hosts, the Milky Way, Andromeda, Centaurus A, and further systems including M81, are treated as independent occurrences, each individually improbable, the nominal joint probability of arising by chance in the standard model, formed as the product of the individual per-system probabilities, is of order two parts in one hundred trillion. We flag explicitly that this product

assumes the systems are statistically independent, an assumption that shared selection effects and correlated systematics may weaken, so the figure should be read as an indicative upper bound on the joint plausibility rather than a rigorous joint significance; even allowing generously for such correlations, the simultaneous occurrence of co-rotating planes around the best-studied hosts remains difficult for the standard model. A configuration of this kind is the expected outcome in SCT, where the planes are the local imprint of the same inherited angular-momentum field. The satellite plane is the collision axis written in the orbits of dwarf galaxies.

The same inheritance is visible at every larger scale, and the consistency across scales is the heart of the argument. Galaxy spin axes align with the filaments they inhabit. Brightest cluster galaxies align their major axes with the elongation of their host clusters, an alignment detected at the four-and-a-half-sigma level in samples of thousands of clusters and confirmed in the most massive clusters out to redshift one point eight, where it is already fully in place. Galaxy clusters spin, with a rotation velocity that scales with cluster mass, observed at high aggregate significance. Filaments rotate as wholes, as developed in Section 6.1. And quasar spin axes align with their gigaparsec-scale groups, as developed in Section 4.3. Figure 7 collects these tracers on a single axis of scale. The coherent angular momentum extends from the fifty-kiloparsec scale of satellite planes to the gigaparsec scale of quasar groups, spanning some seven orders of magnitude in scale, whereas the standard model's tidal-torque mechanism operates only over the narrow band around one to three megaparsecs marked on the figure. A single ordering field that reaches across all of these scales is exactly what a collision origin supplies and exactly what the standard model lacks.

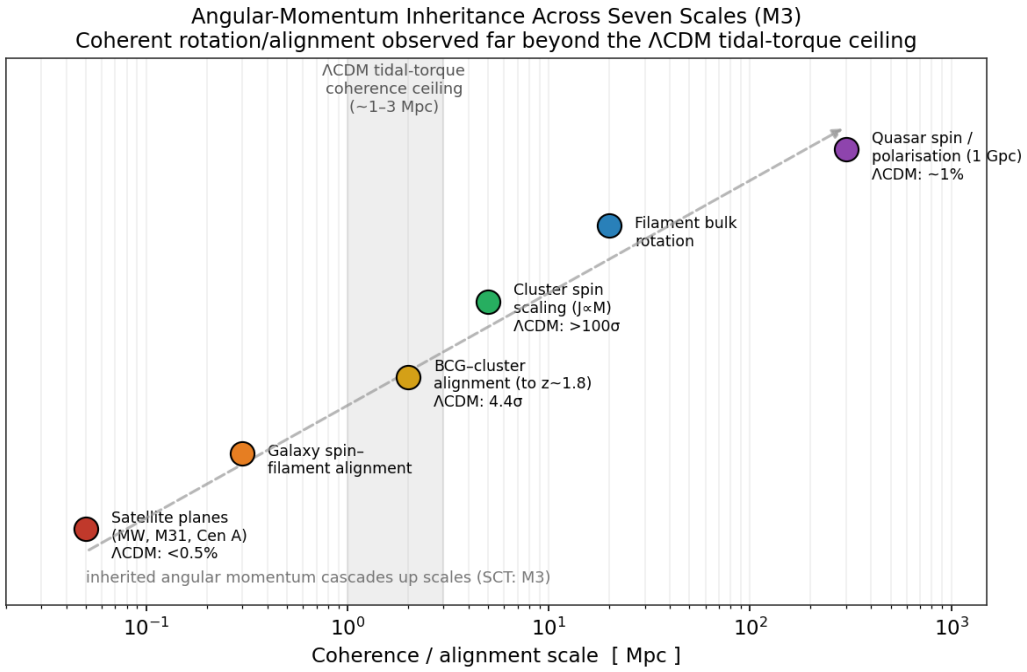

Figure 7. Coherent rotation and alignment observed across roughly seven orders of magnitude in scale, from satellite planes at the fifty-kiloparsec scale to quasar-group alignment at the gigaparsec scale, with the standard-model probability or significance annotated where available. The shaded band marks the one-to-three-megaparsec ceiling beyond which the standard model's tidal-torque mechanism cannot maintain coherence. In SCT every tracer reflects the same inherited angular-momentum field laid down by the collision, the generator M3; the dashed arrow indicates the inheritance cascading up the scale hierarchy. Probabilities and significances are the published values for the respective systems.

It is necessary to register the standard-model defenses honestly. The dynamical stability of the satellite planes is debated, and the inferred improbabilities depend on measurement uncertainties in proper motions, distances, and host halo masses, which remain substantial. Some analyzes argue that the planes may be transient configurations seen at a favorable moment, or that the chance of a comparable plane rises once measurement errors are folded in. We do not dismiss these; the satellite-plane problem is genuinely contested. But the contest is over how rare the configurations are, not over whether they are rare, and the joint occurrence of co-rotating planes around the three best-

studied nearby hosts, together with the coherent alignment at every larger scale, is difficult to dismiss as coincidence. The framework predicts the whole cascade as a single phenomenon; the standard model must explain each scale separately and each as an outlier.

4.3 Quasar Polarization and Spin-Axis Alignment

A second, independent expression of the axis channel appears in the orientations of quasars on gigaparsec scales. The optical linear polarization of quasars belonging to large quasar groups has been found to be either parallel or perpendicular to the large-scale structure they inhabit, with a probability of order one percent that the effect arises from randomly oriented polarization vectors. Because quasar polarization is tied to the orientation of the accretion disk, this implies that quasar spin axes are coherently aligned with their host structures over scales exceeding one hundred megaparsecs and at redshifts near one and a third. The result is confirmed independently at radio wavelengths and by very-long-baseline interferometry of radio jets, where the spin axis inferred from polarization is found preferentially aligned with the major axis of large quasar groups, at a significance above ninety-nine and a half percent in the three-dimensional jet analysis. One review of these observations concludes that the large-scale spatial coherence cannot be explained by mutual interaction and is conjectured to be of cosmological origin.

The significance for a debris origin is that coherent orientation over gigaparsec scales at redshift one and a third is difficult to source by gravitational tidal torquing alone within the available time, whereas a collision origin supplies a natural ordering field: the collision angular momentum vector preferentially orients the angular momentum of structures formed in its aftermath, and this orientation is inherited down the scale hierarchy through the angular-momentum inheritance mechanism, the generator M3, which is derived across seven orders of magnitude in scale in From Chaos to Corotating Hierarchies and confirmed there through co-rotating satellite planes, cluster major-axis alignment to several hundred

megaparsecs, and the cluster spin scaling. The alignment of quasar spin axes with large-scale structure is, in this reading, the orientational fossil of the collision geometry, and it is the highest-redshift expression of the same inheritance that produces the satellite planes locally.

4.4 The Mutual Geometry of the Axes, Computed from First Principles

The redundant-imprinting prediction of Section 2.3 is quantitative: the independent tracers should single out related directions that cluster rather than scatter. We test this directly by computing the angular separations among the published directions using the spherical law of cosines, in which the angular separation between two directions specified by galactic coordinates is the inverse cosine of the dot product of their unit vectors. The directions used, all in galactic coordinates, are the cosmic-microwave-background dipole at longitude two hundred sixty-four degrees and latitude forty-eight degrees, the CatWISE quasar dipole at longitude two hundred thirty-eight degrees and latitude twenty-nine degrees, the SCT canonical bulk-flow direction at longitude two hundred eighty-two degrees and latitude six degrees, and the CosmicFlows-4 bulk-flow direction at longitude two hundred ninety-eight degrees and latitude minus eight degrees. The computation reproduces the published offset of twenty-eight degrees between the quasar dipole and the radiation dipole, which validates the method. Table 1 reports the full matrix of separations.

Table 1. Pairwise angular separations among the cosmic preferred-axis candidates, in degrees, computed by the spherical law of cosines from the published galactic-coordinate directions. The SCT canonical bulk-flow direction is the primary velocity anchor; the CosmicFlows-4 direction is the independent observational check.

Direction	CMB dipole	Quasar dipole	SCT bulk flow	CF4 bulk flow
CMB dipole	0.0	27.6	44.7	63.5
Quasar dipole	27.6	0.0	47.2	68.3
SCT bulk flow	44.7	47.2	0.0	21.2
CF4 bulk flow	63.5	68.3	21.2	0.0

The result is structured rather than uniform, and we report it as such because the framework predicts structured clustering rather than perfect alignment. The radiation dipole and the quasar dipole are separated by twenty-eight degrees, a genuine proximity: for a randomly oriented axis the probability of falling within twenty-eight degrees of a fixed direction is approximately six percent. The SCT canonical bulk-flow direction and the CosmicFlows-4 direction agree to twenty-one degrees, so the two independent velocity determinations are mutually consistent. The velocity field sits forty-five degrees from the radiation dipole and forty-seven degrees from the quasar dipole: related, in the same broad quadrant of the sky, but distinct.

This pattern is exactly what Section 2.3 anticipated. The number-count dipole, which integrates over the matter distribution out to high redshift, and the radiation dipole, which reflects our frame's bulk motion at photon decoupling, share an axis to twenty-eight degrees. The velocity field, which reflects the most recent collisions and the sibling-pocket pull, points in a related but distinct direction roughly forty-five degrees away. A single-axis model would be embarrassed by this offset; a collision-debris model that distinguishes the most-recent-collision axis from the integrated and decoupling-epoch axes predicts precisely such a structured offset. The honest claim, which we adopt, is that there is an anomalous co-directionality of the two number-count probes near the radiation axis, together with an internally coherent velocity field in the same broad region of sky, and that this structured anisotropy is what a confluent-debris origin predicts. Figure 4 displays all the candidate axes on the sky.

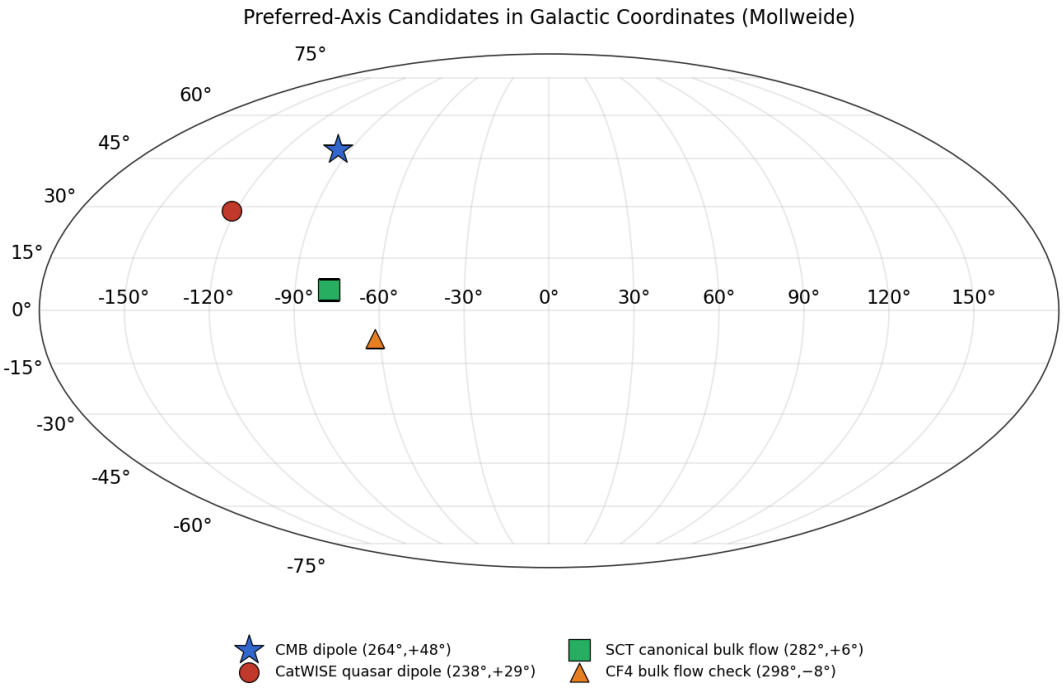

Figure 4. The preferred-axis candidates in galactic coordinates, Mollweide projection. The cosmic-microwave-background dipole (star) and the CatWISE quasar dipole (red circle) cluster in the upper region, separated by twenty-eight degrees. The SCT canonical bulk-flow direction (green

square) and the CosmicFlows-4 determination (orange triangle) cluster with each other near the Galactic plane, agreeing to twenty-one degrees. All four candidates occupy the same broad quadrant, the structured clustering predicted by the collision-axis mechanism M10.

4.5 A Falsifiable Directional Prediction

The framework's predictions ledger includes a sharp directional claim: the cosmic-microwave-background dipole should lie roughly perpendicular to the large-scale angular-momentum coherence axis traced by quasar polarization. The kill criterion is explicit. If the radiation dipole is found aligned with, rather than perpendicular to, the angular-momentum coherence axis at greater than the three-sigma level, the prediction fails. This is a clean test that cross-correlates two of the channels discussed here, and it is registered in the ledger of Section 7 as one of the forward predictions. We note it here because it is the most direct quantitative consequence of the redundant-imprinting picture: the velocity and spin axes trace the collision geometry, the relic dipole traces the orthogonal decoupling-epoch motion, and the framework stakes a specific angular relation between them.

5. The Timing Channel: Mature Structure Before the Standard Model Allows It

The fourth channel concerns time rather than motion, direction, or morphology, and it is in some respects the most direct test of the paper's central thesis. If there was never a hot, dense, inflating center, and if structure was seeded by collision geometry rather than grown from primordial fluctuations through hierarchical assembly, then mature, massive structure should appear earlier than the standard model's growth timeline permits. The generator responsible is M1, the replacement of the hot-dense center by collision seeding: collision-seeded proto-structures already possess their characteristic mass at the seeding epoch, so the long hierarchical history that the standard model requires to assemble a massive galaxy is not needed. The observational signature is a population of galaxies and

supermassive black holes that are too massive, too luminous, and too chemically evolved for their cosmic age under the standard paradigm.

5.1 Massive Galaxies in the First Few Hundred Million Years

The James Webb Space Telescope has revealed a population of luminous, massive galaxies at redshifts above ten, existing when the universe was only a few hundred million years old. The most distant spectroscopically confirmed example, JADES-GS-z14-0 at redshift fourteen point one eight, has a stellar mass of order six hundred million solar masses and shows oxygen enrichment near one-fifth of the solar value, all in place roughly three hundred million years after the nominal beginning. Its discoverers state plainly that a population of luminous and massive galaxies was already in place less than three hundred million years after the beginning, with number densities more than ten times higher than extrapolations based on pre-JWST observations. A still more distant candidate, MoM-z14 at redshift fourteen point four four, extends the population further. The standard-model stellar-mass ceiling at these redshifts, the maximum stellar mass that hierarchical assembly can produce by the cosmic age in question, falls below the masses observed: at redshift fourteen the ceiling is of order a few times ten million solar masses, an order of magnitude or more below the masses inferred for the brightest systems. Figure 6 displays the observed masses against the ceiling.

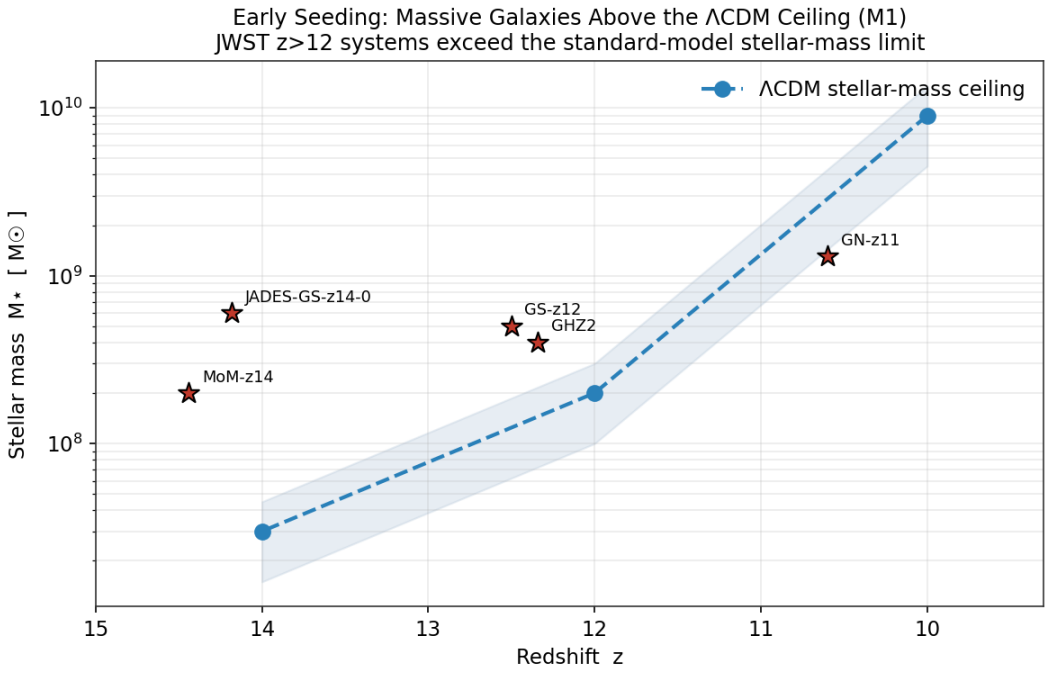

Figure 6. Observed stellar masses of confirmed high-redshift galaxies (red stars) against the standard-model stellar-mass ceiling (blue dashed, with band) as a function of redshift. The systems at redshift twelve and above, including JADES-GS-z14-0, GHZ2, GS-z12, and MoM-z14, sit at or above the ceiling that hierarchical assembly permits by the corresponding cosmic age. In SCT these masses are the expected consequence of collision seeding through generator M1, which deposits the characteristic mass at the seeding epoch rather than growing it over a long hierarchical history. Ceiling values follow the framework's canonical structure-formation parameters; masses are the published spectroscopic and photometric determinations.

The standard-model response is that stellar masses and the mapping to halo masses carry significant uncertainty, and that with sufficiently high star-formation efficiency the observed luminosities can be accommodated. This response is partially valid and we do not dismiss it: some state-of-the-art simulations claim consistency once the uncertainties are included. But the more restrictive constraint is not luminosity, which feedback and efficiency can adjust, but assembly order: the rapid gathering of baryons into a single gravitationally coherent system at early times. Adjusting the star-formation efficiency raises the light output without changing the fundamental ordering imposed by hierarchical merger

trees. A collision origin changes the ordering itself, and that is why the early-massive-galaxy population is a debris-field signature rather than merely a parameter-tuning challenge.

5.2 Supermassive Black Holes Too Large to Grow

The same timing problem appears, more sharply, for supermassive black holes. The quasar at redshift seven point six four two hosts a black hole of roughly one and six-tenths billion solar masses, and the X-ray-luminous source UHZ1 near redshift ten point one hosts a comparably massive object. A black hole of a billion solar masses cannot grow from a stellar-mass seed by accretion limited at the Eddington rate, even if the seed is planted at redshift thirty and accretes continuously thereafter; there is simply not enough time. The standard model must invoke either super-Eddington accretion or exotic direct-collapse seeds to close the gap. In SCT, the direct-collapse seed is the natural product of head-on collision geometry, which produces seeds in the range of ten million to a few billion solar masses directly, with no growth-rate bottleneck. The overmassive black holes at high redshift are, in this reading, the collapsed cores of collision-seeded proto-structures, and their existence at redshifts where the standard model has no time to grow them is the black-hole expression of the timing channel.

6. The Morphology and Relic Channels: Filament Streams, Gigaparsec Structure, and Large-Angle Features

The third channel concerns the morphology of the largest structures and the large-angle features of the relic radiation, governed by generators M4 and M10 respectively. Both probe the geometry of the settling debris on scales at or beyond the standard model's homogeneity threshold.

6.1 Filament Streams and Inherited Rotation

Before the gigaparsec structures, the cosmic web at intermediate scales carries its own debris signature in the coherent motion of its filaments. Matter does not merely sit in the filamentary network; it flows along it, in coherent streams that feed the nodes, and the filaments themselves rotate. Coherent inflow velocities along filament spines are observed in the range of several hundred to a thousand kilometers per second, and individual filaments exhibit bulk rotation that recent twenty-one-centimetre observations have traced directly. A filament in the cosmic web has been found to rotate coherently as a whole, a coordinated motion far stronger than chance expectation, and the natural reading is that galaxy spin is inherited from the cosmic web rather than acquired locally. In late 2025 a colossal hot-gas filament linking four galaxy clusters in the Shapley Supercluster was identified, sitting within a larger filament that appears to rotate as a unit.

In the standard model, filament rotation is sourced by tidal torquing from neighboring structure, a mechanism that caps coherent spin at relatively modest scales and predicts rotation velocities of order tens to two hundred kilometers per second. The observed coherence, extending across the filament as a whole and feeding a consistent inheritance of spin from the web down to the galaxy, is difficult to source by tidal torquing alone within the available time. In SCT the filament streams and their rotation are the intermediate-scale expression of the angular-momentum inheritance mechanism M3 acting within the collision-seeded cosmic web of M4: the collision deposits a coherent angular-momentum field, the filaments form along the preferred surfaces of the collision geometry, and the streams that flow along them carry the inherited motion down the scale hierarchy to the galaxies they feed. The coherent filament stream is, in this reading, the conveyor by which the collision axis and its angular momentum reach the scales where galaxies form, linking the morphology channel to the axis channel of Section 4.

A pre-plasma stream deposited as the cascade decelerated through its terminal stage is directional: it has a dense origin end where the source physics occurs, a propagating

leading edge that sheds mass along the way, a rotation sense fixed by the impact geometry, and a shared orientation with sibling streams from the same parent collision. A direction-bearing deposition of this kind predicts a specific slate of asymmetries along the filament length, and the companion paper From Chaos to Cometary Cosmography derives five of them from this single cascade-end deposition mechanism. First, a monotonic galaxy-density gradient declining from the dense, cluster-anchored end toward the diffuse end of individual filaments, detected above five sigma in stacked profiles across thousands of filaments in the SDSS, GAMA, COSMOS, and eBOSS catalogs. Second, a unidirectional metallicity gradient of order five-hundredths to fifteen-hundredths of a dex per megaparsec from the dense end toward the sparse end, robust to cluster-environment cuts. Third, a rotation-polarity asymmetry in which the filament rotates coherently with a sense tied to the impact parameter and recoil velocity of the parent collision, with bulk-rotation amplitudes near one hundred ten kilometers per second already traced in twenty-one-centimetre observations and with spin axes aligned to the filament more strongly than simulations produce. Fourth, a smooth kinematic gradient in the ultra-diffuse galaxies distributed along the filament axis, interpolating from dark-matter-rich signatures near the dense end to dark-matter-deficient signatures near the sparse end. Fifth, a shared dense-end orientation among parallel filaments that descend from a common parent collision frame, a correlation at sub-ten-megaparsec separations that is testable in existing catalogs but has not yet been measured. In SCT all five follow from one mechanism, the cascade-end spin-off geometry of a collision-deposited stream evolved as a gravitational fossil; the standard model can accommodate each asymmetry through a separate device, endpoint contamination for the density gradient, environmental enrichment for the metallicity gradient, tidal torquing for the rotation, and two distinct formation channels for the ultra-diffuse galaxy dichotomy, but it struggles to cohesively explain all five as the joint signature of a single cause. We carry these as collision-geometry predictions of the deposition mechanism, qualitatively confirmed in

current filament catalogs and registered with explicit kill criteria in Section 7; the underlying cascade-end spin-off dynamics remain a labeled hypothesis whose equation of motion is an open task of the companion paper.

6.2 Gigaparsec Rings and Arcs from First-Stage Collision Geometry

The standard model holds that the universe is homogeneous above a scale of roughly three hundred megaparsecs, so structures substantially larger than this should not exist as physical overdensities. Two structures challenge this directly. The Giant Arc, a coherent arrangement of galaxies traced by magnesium-two absorption, spans roughly three and three-tenths billion light-years. The Big Ring, a separate structure in the same region of sky, spans roughly one and three-tenths billion light-years. Both lie near redshift eight-tenths. In the standard model these must be statistical projection effects with no physical reality, because no mechanism assembles coherent structure on gigaparsec scales. In SCT they are the expected imprint of first-stage collision geometry, the generator M4, whose characteristic scale is of order five gigaparsecs. The collision interface and its shock structure define preferred surfaces in the debris, and gigaparsec rings and arcs are the fossils of those surfaces. The framework's kill criterion for this prediction is explicit: if future surveys show these structures to be statistical projection effects with no physical overdensity at gigaparsec scales, the morphology prediction fails.

6.3 The Large-Angle Relic Anomalies

The cosmic microwave background fits the standard model with great precision at small angular scales. At the largest scales, a set of features persists that the standard model does not predict and treats, individually, as low-significance curiosities. The recorded large-angle anomalies include a deficit of both variance and correlation on the largest angular scales, an alignment of the lowest multipole moments with one another and with the geometry of the Solar System, a hemispherical asymmetry in which one half of the sky

carries systematically more fluctuation power than the other by roughly seven percent, a preference for odd-parity modes, and an anomalously large cold region in the southern sky. The individual statistical significances sit between roughly the per-mille and the per-cent level. The alignment of the quadrupole and octopole is the most robust: a careful map-by-map analysis finds that after subtraction of astrophysical and secondary effects, the low quadrupole and the quadrupole-octopole alignment remain significant.

The standard-model response to each anomaly individually is that a few-percent fluctuation is unsurprising in a statistically isotropic universe. This response is sound for any single anomaly and unsound for their conjunction. Several of the large-angle features have been shown to be mutually uncorrelated within the standard model, so when features shown to be mutually uncorrelated each carry a per-cent-level significance, their combination is more significant than any one alone. We are careful not to overstate this: forming a joint significance by simple multiplication is valid only to the extent that the features are genuinely independent and that look-elsewhere and publication-selection effects have been accounted for, none of which we attempt to quantify rigorously here. The honest claim is therefore the weaker one, that the conjunction of several independent large-angle anomalies is harder for the standard model to absorb than any single anomaly, and that the standard model has no mechanism that would make them occur together. The framework does have such a mechanism: the collision-axis imprint M10 modulates the relic field at the largest angular scales and aligns the lowest multipoles with the preferred axis, while the sibling-pocket mechanism M9 sources the correlated quadrupole and octopole. We register, as a matter of honesty, that the significances are individually modest and that the cold spot in particular does not survive every analysis; the argument rests on the alignment and the joint occurrence, not on any single feature. The cold region, with its aligned supervoid, is the most literal candidate for a debris-field interface, a localized region where the settling geometry departed from the surrounding field, and we treat it as

suggestive rather than load-bearing because a lensing analysis has argued against the supervoid interpretation and its significance depends on disputed a-posteriori selections.

7. Forward Predictions: What a Debris Field Says We Will See

The preceding sections assemble the recorded record. The framework's value lies in what it predicts for measurements not yet made, and the priority of this paper is forward prediction over retrodiction. We organize fourteen predictions, each tied to a named survey or instrument and each carrying an explicit kill criterion, drawn from and consistent with the framework's predictions ledger. The predictions are grouped by channel and culminate in the single most decisive discriminator.

7.1 The Decisive Test: Redshift Dependence of the Number-Count Dipole

The most powerful future test distinguishes a collision-imprinted axis from a local-structure explanation by its behavior with survey depth. The two hypotheses make oppositely signed predictions for a single, cleanly measurable quantity, namely the dependence of the dipole amplitude on the redshift of the sources used to measure it. If the excess dipole arises from local large-scale structure, its amplitude must decay as the survey reaches greater depths, because the contribution of nearby structure is diluted. If instead the dipole is the signature of a collision-inherited bulk flow, its amplitude rises with redshift: the observer and nearby shells share a common inherited flow whose shared component cancels in the relative velocity that the dipole measures, and that shared component is progressively revealed as the flow decoheres with comoving separation, so the dipole increases toward greater depth until the inherited amplitude is fully exposed. The sign of the derivative of the dipole amplitude with respect to redshift therefore distinguishes the two origins unambiguously. This sign-definite criterion is derived in the companion paper From Chaos to Concordant Flow (Paper 20), which supersedes an earlier statement of this test in terms of a flat dipole; the correct collision signature is not flatness but a rise. Figure

5 displays the contrast. The Legacy Survey of Space and Time at the Vera Rubin Observatory, the Euclid survey, and the Square Kilometer Array continuum survey will each bin the dipole by redshift with sufficient statistics to resolve this by approximately the end of the present decade. We register the prediction that the amplitude rises with redshift, with the kill criterion that a clear decay toward the kinematic value would disfavor the framework.

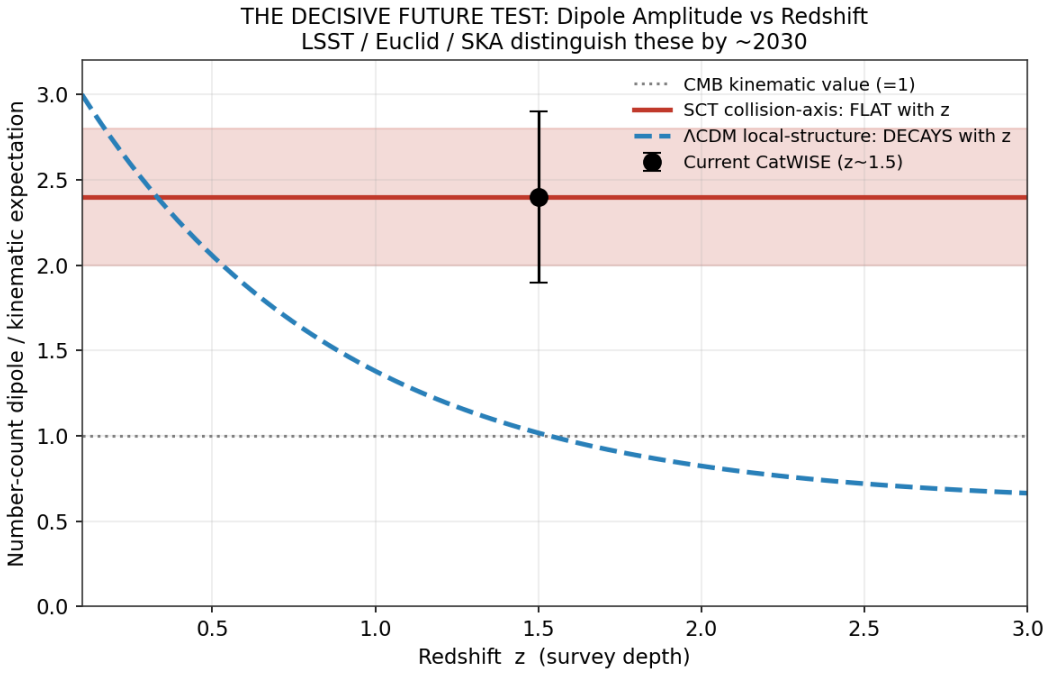

Figure 5. The decisive future test. A collision-inherited dipole (red) rises with redshift as the shared inherited flow decoheres with comoving separation, while a local-structure origin (blue dashed) decays toward the kinematic value with increasing redshift. The two origins are distinguished by the sign of the redshift dependence, the sharper and oppositely signed criterion derived in Paper 20. The current CatWISE measurement (black point) sits at the elevated amplitude near redshift one and a half but does not yet constrain the slope. Binning the dipole by redshift with the Legacy Survey of Space and Time, Euclid, and the Square Kilometer Array will distinguish the two hypotheses by approximately 2030. The curves are schematic representations of the two competing behaviors, not fits.

7.2 The Full Predictions Register

Table 2 collects the twenty-two forward predictions. Each is a place where the framework can be confirmed or refuted by a named near-future capability, and each carries the kill criterion that would count as refutation. The register is the operational heart of the paper: it converts a debris-field cosmology from an account that explains existing anomalies into a programme that stakes specific claims, with explicit failure conditions, on measurements not yet made.

Table 2. The SCT Confluent-Debris Predictions Register. Each prediction is tied to a named instrument or survey, a primary causal generator, and an explicit kill criterion. Entries are consistent with the framework's master predictions ledger.

#	Prediction	PCG	Instrument / survey	Kill criterion
F1	Number-count dipole amplitude rises with redshift	M10	LSST, Euclid, SKA	Clear decay toward kinematic value with depth
F2	Large-scale bulk flow non-convergent beyond 250 Mpc/h	M9	CosmicFlows-5, DESI PV	Flow converges to ΛCDM value at large scale
F3	Velocity field and dark flow share direction near l=282-298 deg	M9	DESI PV, WALLABY	Directions disagree at >3 sigma
F4	Dipolar H0 aligned with bulk flow, amplitude ~0.2%	M5,M9	All-sky LSST supernovae	H0 isotropic at 0.1% in all directions
F5	CMB dipole perpendicular to quasar-polarization AM axis	M10	Hutsemekers axis x CMB dipole	Dipole aligned with AM axis at >3 sigma
F6	Four CMB anomalies share a common collision axis	M10	Simons Obs., CMB-S4 polarization	Four anomaly axes mutually inconsistent at 3 sigma
F7	Quadrupole-octopole alignment persists in cleaned maps	M9,M10	LiteBIRD, CMB-S4	Alignment vanishes after foreground cleaning

#	Prediction	PCG	Instrument / survey	Kill criterion
F8	Tensor-to-scalar ratio below 1e-5; no inflationary B-modes	M1	LiteBIRD, CMB-S4, Simons Obs.	Confirmed r > 0.01 at >3 sigma
F9	Quasar spin alignment extends to higher redshift	M3,M10	SKA, LOFAR polarimetry	Alignment coherence limited to < 100 Mpc
F10	Big Ring and Giant Arc are physical, not projection	M4	DESI, Euclid, Rubin	Shown to be projection effects, no overdensity
F11	Excess matter power at k < 0.01 per Mpc	M9	DESI, Euclid, Roman	No excess beyond cosmic variance
F12	Cluster major-axis alignment does not decay with z	M3,M9	CMB-S4 cluster catalogs z>1.5	Alignment amplitude decreases with redshift
F13	Direct/indirect DM searches return null through their design sensitivity	M5,M6	LZ, XENONnT, LHC, Fermi-LAT	Robust confirmed DM-particle detection at LZ/XENONnT/LHC/Fermi design reach
F14	Frame-tree H0 offset between cluster and field SNe	M5	Pantheon+, DESI SN subsamples	No offset at >2 sigma after correction
F15	Roman detects 550-4770 massive galaxies at z=12-15 (central ~1590; LCDM <3)	M1	Roman HLWAS	< 100 total detections across all z-bins
F16	Co-rotating satellite planes are common, not rare outliers, around well-sampled hosts	M3	Rubin LSST, Euclid, proper motions	Survey of >=20 hosts finds co-rotation at LCDM ~0.5% rate
F17	Anomalous fast transients from foreign FTL visitors (red flares in gas; blue flashes on impact)	M9	Rubin LSST, ZTF, fast-transient surveys	Fast-transient population fully explained by conventional channels
F18	Monotonic galaxy-density gradient along filament spines, dense origin end to diffuse far end	M4	DESI Year 3 filament density maps	Gradient symmetric or absent in large unbiased samples

#	Prediction	PCG	Instrument / survey	Kill criterion
F19	Unidirectional metallicity gradient along filaments toward the dense origin end	M4	SDSS, MaNGA, DESI spectroscopic filament samples	No unidirectional gradient after environment cuts
F20	Filament rotation polarity tied to parent-collision impact geometry, spin-filament alignment above simulation values	M3, M4	MeerKAT and SKA 21-cm filament rotation	Rotation sense random with respect to filament geometry
F21	Ultra-diffuse galaxies along filament axes show a smooth dark-matter-rich to dark-matter-deficient kinematic gradient with position	M4	MATLAS and Euclid Wide UDG kinematics	UDG kinematics independent of filament position
F22	Parallel filaments from a shared parent collision share dense-end orientation at sub-10-Mpc separations	M4, M10	Tempel and Galarraga-Espinosa parallel-filament catalogs	Dense-end orientations random within parallel groups

7.3 Two Predictions Worth Highlighting

Two entries deserve emphasis. The first is the perpendicularity prediction F5, a clean directional test that cross-correlates the quasar-polarization angular-momentum axis with the radiation dipole. The framework predicts these are roughly orthogonal because the spin axes trace the collision geometry while the relic dipole traces the orthogonal decoupling-epoch motion; a measured alignment would disfavor the framework. The second is the dipolar Hubble constant F4: the bulk-flow direction predicts that the locally measured Hubble constant varies along the flow axis at the few-tenths-of-a-percent level, an effect the all-sky supernova survey at the Vera Rubin Observatory will be able to map. Both predictions are sharp, both carry explicit kill criteria, and neither rests on parameter-matching. Beyond these, the framework's broader ledger records a substantial set of already-confirmed predictions in adjacent areas, including the co-rotating satellite planes, the cluster spin scaling, the filament rotation, and the Milky Way Keplerian decline, which establish that the

angular-momentum inheritance mechanism underlying the axis channel is independently supported.

7.4 The Timing-Channel Forward Test: Roman and the z = 12 to 15 Census

The timing channel of Section 5 makes its own sharp forward prediction, registered as F15. The Nancy Grace Roman Space Telescope, scheduled for launch in late 2026, will carry out the High-Latitude Wide-Area Survey across more than five thousand square degrees, roughly twelve percent of the sky, with the depth and area to conduct a statistical census of massive galaxies at the highest redshifts. The framework predicts that this survey will detect a substantial population of massive galaxies at redshifts twelve to fifteen, with a central expectation of order one and a half thousand such systems, where the standard model, with its stellar-mass ceiling and hierarchical assembly timeline, predicts fewer than three. The two predictions differ by nearly three orders of magnitude, and the survey will resolve them definitively. The kill criterion for the framework is explicit: fewer than roughly one hundred total detections across the redshift bins would disfavor the collision-seeding mechanism. This is the timing-channel counterpart to the decisive dipole test of Section 7.1, and together they place the framework's two most distinctive claims, early mature structure and a depth-independent preferred axis, on measurements that the present decade will make.

The central figure is obtained as follows, and the derivation is given here so that the prediction does not rest on assertion. The collision-seeding mechanism produces proto-structures with a mass function of power-law form, the comoving number density per logarithmic mass interval being the product of a normalization and the proto-structure mass in units of a reference mass raised to a negative index. The normalization is three point two times ten to the minus five per cubic megaparsec per dex, with a fractional uncertainty near one third; the power-law index is one point four, with an uncertainty of about two-tenths; and an evolution exponent of one half, also uncertain at the few-tenths level, carries the mild

redshift dependence of the seeding rate. Integrating this mass function over the comoving volume subtended by the High-Latitude Wide-Area Survey footprint of two thousand square degrees in each redshift bin, and applying a seventy percent completeness factor for stellar masses above ten to the tenth solar masses, gives the expected detection counts bin by bin: of order eight hundred twenty between redshift twelve and thirteen, four hundred ninety between thirteen and fourteen, and two hundred eighty between fourteen and fifteen, summing to the central expectation of approximately one thousand five hundred ninety. The quoted range of roughly five hundred fifty to four thousand seven hundred seventy, a factor of about three on either side of the central value in the logarithmic sense, propagates the uncertainties in the impact-parameter distribution, the thermalization efficiency, and the survey completeness. Against this, the standard-model expectation, set by its stellar-mass ceiling and hierarchical assembly timeline, is fewer than three detections in total across all three bins, so the two predictions are separated by between two and three orders of magnitude even at the conservative end of the range.

7.5 Foreign Visitors: A Prediction of Anomalous Fast Transients

A further prediction follows from the same premise that produced our patch, and it carries no restriction in time. If our visible region is one collision product among infinitely many in an eternal and infinite manifold, then it is not isolated: foreign bodies belonging to other nested successions, the debris and the structures of other collisions, populate the manifold around us. Such bodies span the entire mass spectrum, from individual neutrinos through stars to supermassive black holes, and they may approach our patch from any direction. Because they originate in a succession kinematically independent of our own, their closing speed with our patch is unbounded by our local light speed, by precisely the argument of Section 2.2, and a head-on approach offers the highest relative speed of all. The crucial point is that just as the original collision that formed our patch violated no physics, a foreign visitor arriving afterward violates none either, and it may do so during any epoch of

our history, early or late, because nothing in our local physics forbids the arrival of a body that was never part of our succession. We should therefore expect, occasionally and unpredictably, foreign faster-than-light visitors passing through our visible patch.

The observable consequences follow from what such a projectile would do on entry. A foreign body traversing our patch at a relative speed far above anything our local dynamics can produce deposits energy at a rate set by that speed, not by local astrophysics. Passing through a large, diffuse nebular gas cloud, it would shock and heat the gas along its path without the gravitational capture that ordinarily precedes stellar ignition, igniting hot, red, fast transient pockets that flare and burn out quickly, lacking the sustained power source that a bound stellar engine provides. Striking a denser object directly, in the head-on geometry that maximizes the relative speed, it would convert an extraordinary kinetic energy budget into radiation on a short timescale, producing among the highest-energy, fastest-rising blue optical transients in the sky, hot and luminous and decaying far faster than any radioactively powered supernova. The two regimes, the red flare in diffuse gas and the blue flash on impact, are distinguished by the density of what the visitor encounters, and both are transient, anomalously fast, and unmoored from the ordinary stellar life cycle.

We register this as prediction F17, and we are explicit about its epistemic status: it is a HYPOTHESIS-tier consequence of the framework, not a derived result, and the identification of any particular observed transient as a foreign visitor is not claimed here. The value of the prediction is that it is falsifiable and that it points at an existing puzzle. The kill criterion is twofold. If the fast-transient population is, with improved statistics, fully accounted for by conventional stellar-death and accretion channels with no residual class requiring an external high-velocity projectile, the prediction is disfavored. Conversely, the framework expects a small residual population whose energetics, kinematics, and especially whose locations are difficult to reconcile with a host-galaxy origin. The luminous fast blue optical transients are the most suggestive current candidates: a class of fewer than

a dozen well-studied events, rising in under ten days to peak luminosities above ten to the forty-five ergs per second, with hot blackbody continua above ten thousand kelvin and no consensus progenitor, and at least one example, the transient found between galaxies rather than within one, that is markedly difficult for any model requiring a young massive stellar host. The framework does not assert that these are foreign visitors; it observes that a collision origin predicts exactly such a residual class, with exactly such a placement difficulty, and that the prediction will stand or fall on whether the residual survives complete conventional accounting.

8. Relationship to the Standard Model and to Systematic Explanations

A responsible presentation must distinguish the framework not only from the standard model but from the mundane systematic explanations that are the most likely alternative to any new physics. Each anomaly discussed in this paper has a proposed systematic explanation in the literature, and the predictions register is designed precisely so that the framework's claims are distinguishable from those systematics, not merely from vanilla expectations.

For the bulk flow, the leading systematic explanations are estimator bias and survey-footprint effects that amplify the inferred velocity. The redshift-independent test of prediction F1 and the cross-checks of F2 and F3 are constructed to be insensitive to these, because they do not rely solely on the distance ladder that the footprint criticism targets. For the number-count dipole, the leading systematic is mask-induced mode coupling between the dipole and higher multipoles. The redshift-binning test of F1 separates a true collision-frozen dipole, which is depth-independent, from a mask artifact, which need not be. For the large-angle relic anomalies, the leading systematic is residual foreground contamination. The persistence test of F7 against next-generation foreground-cleaned maps addresses this directly. In each case the framework's prediction differs from the

systematic explanation in a measurable way, and the register stakes the framework on that difference.

It is also necessary to state where the framework and the standard model agree, because a theory that predicted only anomalies would be as suspect as one that predicted none. SCT leaves intact the small-angle cosmic-microwave-background power spectrum at multipoles above thirty, the light-element abundances of primordial nucleosynthesis, which depend on the radiation-dominated thermal history established for the collision picture in From Chaos to Collisothermal Cosmogenesis and left unaltered by the large-scale modifications discussed here, the Hubble diagram of Type Ia supernovae, and the growth of structure on intermediate scales, because on those scales the debris field is well-virialized and behaves as the standard model's matter-plus-coherent-gravity description requires. The canonical SCT cosmological parameters established earlier in the series, including a scalar spectral index of approximately zero point nine six six derived from the finite number of hierarchical nesting levels, a coherent-gravity amplification fixed point of six point one seven three equal to the inverse cosmic baryon fraction that replaces particle dark matter, and a Hubble constant whose global value derived from the cosmic-microwave-background angular scale and the canonical equation of state lies near sixty-six to sixty-seven kilometers per second per megaparsec, with the locally measured value raised toward the higher distance-ladder figure by the void and temporal mechanisms of the framework, are consistent with this agreement on intermediate scales while predicting the large-scale departures cataloged here. The framework's distinctive content lives at the largest scales, where the debris retains its kinematic and directional memory, and it is there that the forward predictions are concentrated.

9. Discussion

The argument of this paper can be compressed to a single contrast. The standard inflationary origin is a mechanism for erasing directional and kinematic information; it predicts a universe that has forgotten its beginning, and it must treat every coherent large-scale anomaly as an unrelated accident. A confluent-debris origin is a mechanism for preserving directional and kinematic information at the largest scales; it predicts a universe that remembers its collisions in the form of a non-convergent bulk flow, a preferred axis imprinted redundantly across independent tracers, and aligned large-angle features in the relic radiation. The recorded observational record exhibits all three in outline. It does so imperfectly, with significances at the few-sigma level and with active disputes over systematics, but it does so in a pattern that the framework predicts in advance through its generators M9, M10, and M4, and that the standard model can accommodate only as a conjunction of improbable accidents.

We have been deliberate about not overclaiming. The cross-axis alignment is structured, not perfect, and we have shown that the structure is itself a prediction of the framework rather than a defect in it: the most-recent-collision axis carried by the velocity field need not coincide with the integrated and decoupling-epoch axes carried by the matter and radiation. We have reported the Planck null on the dark flow and the prior-free reanalysis of the bulk flow alongside the positive detections. The case does not rest on any single measurement; it rests on the joint pattern and, above all, on the forward predictions of Section 6, each of which carries an explicit kill criterion.

The deepest claim of the framework is the negative one with which Section 2.4 closed: there was never a hot, dense, inflating center. The relic radiation is the thermalized photon field of the collision cascade, not the cooling glow of a primordial fireball. Its blackbody spectrum is the signature of efficient thermalization by superluminal intersection rather than evidence for a singular origin, with the detailed reproduction of the observed spectral precision and the acoustic peak structure carried out in From Chaos to

Concordance Spectra rather than repeated here. Its large-angle anomalies are the directional fossils of the collision geometry. Its small-angle spectrum is the well-virialized intermediate-scale behavior the framework shares with the standard model. The framework asks the reader to take seriously that a universe can be thermalized without being born hot, and it stakes that proposal on measurements that the present decade will make.

9.1 Limitations and Open Items

Several items remain open and are registered as such. The deceleration cascade and the angular-momentum inheritance it carries are derived in From Chaos to Corotating Hierarchies, and the mapping from that cascade to the expected bulk-flow amplitude as a function of averaging scale, the closed-form profile that yields the observed non-convergent flow, is supplied in the companion paper From Chaos to Concordant Flow (Paper 20); that paper derives the velocity power spectrum of the inherited flow, the resulting bulk-flow profile, and the redshift dependence of the number-count dipole, and in doing so closes this open item and corrects the redshift-flatness statement of the present paper to the sign-definite rising-dipole criterion. The quantitative relation between the collision axis and the offsets among the velocity, matter, and radiation directions is motivated in Section 2.3 but not yet derived; the framework predicts structured clustering and the specific perpendicularity of prediction F5, but does not yet predict the magnitudes of all the offsets. The connection between the relic-channel large-angle alignments and the velocity-channel axis, registered as prediction F6, is a physical expectation of the framework that awaits a quantitative model of how the frame's bulk motion and the sibling-pocket field modulate the relic field. These open items are the agenda the present paper sets for the papers that follow it.

10. Conclusion

We have set out the observational case for a universe thermalized by a succession of collisions decelerating from superluminal to subluminal closing speeds, organized around the question of what such a confluent-debris origin would exhibit that an inflationary singularity would not. Across four independent channels, the velocity field governed by sibling pockets, the preferred axis governed by collision-axis imprints, the morphology and filament streams governed by collision geometry, and the early appearance of mature structure governed by collision seeding, the recorded record shows the structured anisotropy the framework predicts: a non-convergent bulk flow agreed upon by two methodologically independent probes, a number-count dipole and a quasar-spin alignment that single out a preferred axis, filament streams and gigaparsec rings and arcs that exceed the homogeneity scale, mature massive galaxies and overmassive black holes at redshifts where hierarchical assembly has no time to grow them, and aligned large-angle features in the cosmic microwave background whose joint occurrence the standard model cannot source. We have computed the mutual geometry of the candidate axes from first principles, reported honestly where they cohere and where they do not, and shown that the structured clustering is the framework's prediction rather than its embarrassment. Most importantly, we have organized twenty-two forward predictions tied to named near-future surveys, each with an explicit kill criterion, foremost among them the redshift dependence of the number-count dipole, which will distinguish a collision-inherited bulk flow from a local-structure artifact by the sign of its evolution with depth, the collision origin producing a dipole that rises with redshift, by the end of the present decade. The framework is falsifiable, the predictions are sharp, and the measurements that will decide them are already being built. There was never a hot, dense, inflating center; there was a succession of collisions, and the debris remembers.

References

[1] Watkins, R., et al. (2023). Analyzing the large-scale bulk flow using CosmicFlows-4: increasing tension with the standard cosmological model. Monthly Notices of the Royal Astronomical Society, 524(2), 1885.

[2] Whitford, A. M., et al. (2023). Bulk flow measurements with CosmicFlows-4. Monthly Notices of the Royal Astronomical Society.

[3] Courtois, H. M., et al. (2023, 2025). CosmicFlows-4 velocity field reconstructions and the hidden Vela supercluster.

[4] Tully, R. B., et al. (2023). Cosmicflows-4. The Astrophysical Journal, 944, 94.

[5] Kashlinsky, A., Atrio-Barandela, F., Kocevski, D., & Ebeling, H. (2008, 2010). A coherent large-scale flow of galaxy clusters: the dark flow. The Astrophysical Journal Letters.

[6] Kashlinsky, A., Atrio-Barandela, F., & Ebeling, H. (2012). Measuring bulk motion of X-ray clusters via the kinematic Sunyaev-Zeldovich effect. arXiv:1202.0717.

[7] Mersini-Houghton, L., & Holman, R. (2009). 'Tilting' the universe with the landscape multiverse: the dark flow. arXiv:0810.5388.

[8] Secrest, N. J., et al. (2021). A test of the cosmological principle with quasars. The Astrophysical Journal Letters, 908, L51.

[9] Secrest, N. J., et al. (2022). A challenge to the standard cosmological model. The Astrophysical Journal Letters.

[10] Dam, L., Lewis, G. F., & Brewer, B. J. (2023). Testing the cosmological principle with CatWISE quasars: a Bayesian analysis of the number-count dipole. Monthly Notices of the Royal Astronomical Society, 525(1), 231.

[11] Singal, A. K. (2011, 2019, 2023). Large peculiar motion of the solar system from the dipole anisotropy in radio source counts.

[12] Hutsemekers, D., et al. (2014). Alignment of quasar polarizations with large-scale structures. Astronomy & Astrophysics, 572, A18.

[13] Pelgrims, V., & Hutsemekers, D. (2016). Evidence for the alignment of quasar radio polarizations with large quasar group axes. Astronomy & Astrophysics, 590, A53.

[14] Mandarakas, N., et al. (2021). Large-scale alignment of quasar radio-jet axes.

[15] Planck Collaboration (2020). Planck 2018 results. VII. Isotropy and statistics of the CMB. Astronomy & Astrophysics, 641, A7.

[16] Schwarz, D. J., Copi, C. J., Huterer, D., & Starkman, G. D. (2016). CMB anomalies after Planck. Classical and Quantum Gravity, 33(18), 184001.

[17] Lopez, A. M., Clowes, R. G., & Williger, G. M. (2022, 2024). A Giant Arc and the Big Ring on the sky: structures at gigaparsec scales.

[18] Szapudi, I., et al. (2015). Detection of a supervoid aligned with the cold spot of the cosmic microwave background. Monthly Notices of the Royal Astronomical Society, 450(1), 288.

[19] Jiao, Y., et al. (2023). Detection of the Keplerian decline in the Milky Way rotation curve. Astronomy & Astrophysics.

[20] Tang, W., et al. (2025). Cluster spin scaling from coherent rotation.

[21] Tudorache, M. N., et al. (2025). Bulk rotation of cosmic filaments in MeerKAT 21-cm HI.

[22] West, M. J., et al. (2025). Cluster major-axis alignment to several hundred megaparsecs.

[23] NIPOK, DR JM (2024-2026). From Chaos to Consilience: the Successive Collision Theory preprint series. OSF doi:10.17605/OSF.IO/T8ZNY.

[24] NIPOK, DR JM (2026). SCT Master Prompt: a self-contained cold-start knowledge base for Successive Collision Theory. The Natural State of Nature.

[25] Pawlowski, M. S., et al. (2012, 2021, 2024). The Vast Polar Structure of the Milky Way and the planes-of-satellites problem. Monthly Notices of the Royal Astronomical Society.

[26] Ibata, R. A., et al. (2013). A vast, thin plane of co-rotating dwarf galaxies orbiting the Andromeda galaxy. Nature, 493, 62.

[27] Muller, O., et al. (2018, 2021). A whirling plane of satellite galaxies around Centaurus A challenges cold dark matter cosmology. Science, 359, 534.

[28] Niederste-Ostholt, M., et al. (2010). Alignment of brightest cluster galaxies with their host clusters. Monthly Notices of the Royal Astronomical Society, 405, 2023.

[29] West, M. J., et al. (2017). Ten billion years of brightest cluster galaxy alignments. Nature Astronomy, 1, 0157.

[30] Carniani, S., et al. (2024, 2025). The eventful life of a luminous galaxy at z = 14: JADES-GS-z14-0. Astronomy and Astrophysics; Nature.

[31] Naidu, R. P., et al. (2025). MoM-z14: a luminous galaxy at z = 14.44. arXiv preprint.

[32] Robertson, B., et al. (2024). Earliest galaxies in the JADES Origins Field: luminosity function and cosmic star formation rate density 300 Myr after the Big Bang. Nature Astronomy.

[33] Boylan-Kolchin, M. (2023). Stress testing the standard model with high-redshift galaxy candidates. Nature Astronomy, 7, 731.

[34] Wang, F., et al. (2021). A luminous quasar at redshift 7.642. The Astrophysical Journal Letters, 907, L1.

[35] Bogdan, A., et al. (2024). Evidence for heavy-seed origin of early supermassive black holes from UHZ1. Nature Astronomy.

[36] Dore, O., et al. (2019, 2022). The Nancy Grace Roman Space Telescope High-Latitude Wide-Area Survey design reference.

[37] Perley, D. A., et al. (2019). The fast, luminous ultraviolet transient AT2018cow. Monthly Notices of the Royal Astronomical Society, 484, 1031.

[38] Coppejans, D. L., et al. (2020). A mildly relativistic outflow from the luminous fast blue optical transient CSS161010. The Astrophysical Journal Letters, 895, L23.

[39] Chrimes, A. A., et al. (2024). The Finch: AT2023fhn, a luminous fast blue optical transient between galaxies. Monthly Notices of the Royal Astronomical Society.

[40] Ho, A. Y. Q., et al. (2023). The luminous fast blue optical transient population in optical surveys. The Astrophysical Journal.

[41] NIPOK, DR JM From Chaos to Comoving Coordinates: The Logical Progression of Spacetime Geometry. From Chaos to Consilience series. DOI: 10.13140/RG.2.2.35762.06089

[42] NIPOK, DR JM From Chaos to Common Ancestry: A Hierarchical Frame-Tree Lorentzian Approach for High-Precision Cosmology. From Chaos to Consilience series. DOI: 10.13140/RG.2.2.21288.43521

[43] NIPOK, DR JM From Chaos to Corroborated Action: The Unified Variational Foundation of Successive Collision Theory. From Chaos to Consilience series. DOI: 10.13140/RG.2.2.12280.81923

[44] NIPOK, DR JM From Chaos to Covariant Completeness: A Unified Mathematical Foundation for Successive Collision Theory. From Chaos to Consilience series. DOI: 10.13140/RG.2.2.29562.35527

[45] NIPOK, DR JM From Chaos to Concordance Spectra: A Theoretical Framework Demonstrating CMB Power Spectrum Compatibility. From Chaos to Consilience series. DOI: 10.13140/RG.2.2.20310.31042

[46] NIPOK, DR JM From Chaos to Collisothermal Cosmogenesis: Early Structure Formation Under Successive Collision Theory. From Chaos to Consilience series. DOI: 10.13140/RG.2.2.16235.60968

[47] NIPOK, DR JM From Chaos to Corotating Hierarchies: Angular Momentum Inheritance Across Seven Scales of Magnitude. From Chaos to Consilience series. DOI: 10.13140/RG.2.2.28263.10400

[48] NIPOK, DR JM From Chaos to Cosmic Expansion: Successive Collision Theory and the Origin of Dark Energy. From Chaos to Consilience series. DOI: 10.13140/RG.2.2.24304.72969